*Plant Biotechnology* 40, 51–62 (2023)
DOI: 10.5511/plantbiotechnology.23.0122a

***Original Paper***

# Molecular characterization of Satsuma mandarin (*Citrus unshiu* Marc.) VASCULAR PLANT ONE-ZINC FINGER2 (CuVOZ2) interacting with CuFT1 and CuFT3

Nazmul Hasan[1], Naoki Tokuhara[2], Takayuki Noda[3], Nobuhiro Kotoda[1,2,3,*]

[1]The United Graduate School of Agricultural Sciences, Kagoshima University, Kagoshima 890-0065, Japan; [2]Graduate School of Advanced Health Sciences, Saga University, Saga 840-8502, Japan; [3]Graduate School of Agriculture, Saga University, Saga 840-8502, Japan
*E-mail: koto@cc.saga-u.ac.jp, nobu_fruits@yahoo.co.jp Tel: +81-952-28-8744

Received December 1, 2022; accepted January 22, 2023 (Edited by R. Hayama)

**Abstract** Shortening the juvenility is a burning issue in breeding fruit trees such as Satsuma mandarin (*Citrus unshiu* Marc.). Decreasing the breeding period requires a comprehensive understanding of the flowering process in woody plants. Throughout the *Arabidopsis* flowering system, FLOWERING LOCUS T (FT) interacts with other transcription factors (TFs) and functions as a transmissible floral inducer. In a previous study, a VASCULAR PLANT ONE-ZINC FINGER1 (VOZ1)-like TF from the Satsuma mandarin, CuVOZ1, showed protein–protein interaction with two citrus FTs in a yeast two-hybrid (Y2H) system and precocious flowering in *Arabidopsis*. In this study, another *VOZ*, *CuVOZ2*, was isolated from the Satsuma mandarin 'Aoshima' and protein–protein interaction was confirmed between CuVOZ2 and CuFTs. No apical meristem (NAM) and zinc coordination motifs were identified within the N-terminal of CuVOZ2. Docking simulation predicted that interactions between CuVOZ2 and CuFTs might occur in domain B of CuVOZ2, which contains a zinc finger motif. According to docking predictions, the distances between the amino acid residues involved ranged from 1.09 to 4.37 Å, indicating weak Van der Waals forces in the interaction. Cys216, Cys221, Cys235, and His239 in CuVOZ2 were suggested to bond with a $Zn^{2+}$ in the Zn coordination motif. Ectopic expression of 35SΩ:*CuVOZ2* in *Arabidopsis* affected the flowering time, length of inflorescence and internode, and number of siliques, suggesting that *CuVOZ2* might regulate both vegetative and reproductive development, act as a trigger for early flowering, and be involved in the elongation of inflorescence possibly in a slightly different way than *CuVOZ1*.

**Key words:** citrus, docking simulation, FLOWERING LOCUS T, transcription factor, yeast two-hybrid.

## Introduction

Citrus accounts for a significant portion of commercially cultivated fruit crops around the globe. The selection of ideal commercial and cultural traits in citrus through traditional breeding methods is time-consuming. A long juvenile period of five to ten years hinders conventional breeding, heredity improvement, genetic studies, and ultimately the production of citrus depending on the species (Albrigo et al. 2019; Krajewski and Rabe 1995). It is still unknown what molecular mechanisms underlie the shifts from the juvenile vegetative to the adult reproductive phase in woody plants like citrus, which might provide clues on how citrus breeding may be accelerated.

In a typical flowering paradigm, *FLOWERING LOCUS T (FT)*, which integrates photoperiod and vernalization pathways, functions as a transmissible floral inducer, similar to florigen, during the transitions from the vegetative to the reproductive phase in *Arabidopsis* (Corbesier et al. 2007; Jaeger and Wigge 2007; Mathieu et al. 2007; Notaguchi et al. 2008). In the companion cells of leaves at dusk, FT is induced by photoperiodic signals through CONSTANS (CO) (Andrés and Coupland 2012; Koornneef et al. 1991; Liu et al. 2013; Mathieu et al. 2007; Samach et al. 2000; Wigge 2011). Induced FT then translocates to the shoot apical meristem (SAM) through the sieve tube system and forms a complex with transcription factors (TFs), inducing expression of the floral meristem identity genes and promoting flowering (Abe et al. 2005; An et al. 2004; Jaeger and Wigge 2007; Lin et al. 2007; Liu et al. 2012; Putterill and Varkonyi-Gasic 2016; Tamaki et al. 2007; Wigge et al. 2005). Another member of the PEBP-like gene family known as *TERMINAL FLOWER1 (TFL1)* functions in the repression of flowering (Bradley et al. 1997; Ohshima et al. 1997). FT and TFL1 contain a potential ligand-binding pocket region within the fourth exon. Ahn et al. (2006) demonstrated that the fourth exon, especially segments B and C in that region, plays a critical role in

Published online March 17, 2023

determining the function of TFL1 or FT in *Arabidopsis*. Our previous study demonstrated a protein–protein interaction of MdVOZ1a, apple VASCULAR PLANT ONE-ZINC FINGER (VOZ) 1, a member of the NAC family subgroup VIII-2 TF, with MdFT1 and MdFT2, two apple FT proteins, in the Y2H system, suggesting the possible involvement of MdVOZ1a in leaf and fruit development through the binding with MdFTs (Mimida et al. 2011).

*VOZ* is a multifunctional gene regulating various biological processes, such as flower induction and development, pathogen defense, and abiotic stress responses (Li et al. 2020). VOZ transcription factors are present exclusively in higher plants, including vascular plants (Mitsuda et al. 2004). In *Arabidopsis*, VOZ1 and VOZ2 have a zinc-finger motif and transcriptional activator activities (Jensen et al. 2010; Mitsuda et al. 2004). *AtVOZ1* is especially expressed in the phloem, whereas *AtVOZ2* is abundantly expressed in *Arabidopsis* roots. Despite the differences in the lengths of the amino acid sequences, molecular weights, and sequence similarities between AtVOZ1 and AtVOZ2, they are redundantly involved in flowering (Celesnik et al. 2013; Kumar et al. 2018; Yasui and Kohchi 2014; Yasui et al. 2012). In addition, it is reported in *Arabidopsis* that the loss-of-function mutation in *VOZ* genes confers cold and drought tolerance but causes growth inhibition, higher temperature and salt sensitivities, and susceptibility to pathogens such as fungi and bacteria (Koguchi et al. 2017; Nakai et al. 2013a; Prasad et al. 2018; Song et al. 2018). In rice, *OsVOZ1* and *OsVOZ2* act as negative and positive regulators, respectively, to resist the fungal pathogen *Magnaporthe oryzae* (Wang et al. 2021). *VOZ*s individually suppress *FLOWERING LOCUS C (FLC)*, a floral repressor, and activate *FT* to promote flowering. Inducing *FT* expression and photoperiodic flowering in *Arabidopsis* also results from the modification of the function of CO protein by VOZs (Koguchi et al. 2017; Kumar et al. 2018; Nakai et al. 2013a, 2013b; Song et al. 2018; Yasui and Kohchi 2014; Yasui et al. 2012). Previous reports suggest that VOZ transcription factors play crucial roles in regulating plant growth and development and have important application values in the genetic improvement of stress resistance in crops.

However, in woody plants, the mechanism of protein–protein interaction between VOZs and FT and further regulation of flowering/fruiting have yet to be investigated. In addition to the protein–protein interaction between MdVOZ1a and MdFTs (Mimida et al. 2011), we recently found the interaction between citrus CuVOZ1 and CuFTs (CuFT1 and CuFT3) in the Y2H system (Hasan et al. 2023). Therefore, in this study, the protein–protein interactions between the other VOZ (CuVOZ2) and CuFTs from the Satsuma mandarin were elucidated with some methods of Y2H, deletion mutation, and docking simulation. The characterization of *CuVOZ2* was also performed using transgenic *Arabidopsis*.

## Materials and methods

### *Plant materials*

The adult vegetative and reproductive tissues of the Satsuma mandarin (*Citrus unshiu* Marc.) 'Aoshima' were collected in 2018 from the Saga Prefectural Fruit Tree Experiment Station in Ogi, Japan as described by Hasan et al. (2023). The juvenile vegetative tissues were collected in August 2019 from 20-month-old seedlings grown at Saga University. Seeds of 'Aoshima' were collected in January 2020. Transgenic *Arabidopsis* plants were grown under long-day (LD) conditions in an incubator (Biotron; Nippon Medical and Chemical Instruments Co., Ltd., Tokyo, Japan). All collected tissues/plants were immediately frozen with liquid nitrogen and preserved in a freezer at −70°C until RNA extraction.

### *Isolation of* CuVOZ2 *from the Satsuma mandarin 'Aoshima'*

Total RNA was extracted from tissues using the cetyltrimethylammonium bromide (CTAB) method (Kotoda et al. 2000). A reverse transcription (RT) reaction was performed using ReverTra Ace® qPCR RT Master Mix FSQ-301 (TOYOBO Co., Ltd., Osaka, Japan) with the extracted RNA from new leaves. The cDNA was amplified from the RT product by polymerase chain reaction (PCR) using KOD Plus Neo (TOYOBO). After attachment of the adenine nucleotide, the amplified PCR products were cloned into pGEM®-T Easy vectors (Promega, Madison, WI, USA). Several clones were sequenced and confirmed using an ABI PRISM 3130xl Genetic Analyzer (Life Technologies, Carlsbad, CA, USA). The isolated genes were designated as *CuVOZ2* (acc. no. LC729265). The oligonucleotide primer sets used in gene cloning are listed in Supplementary Table S1.

### *Phylogenetic analysis and comparison of amino acid sequences*

Putative amino acid sequences were analyzed using the ClustalX2 multiple-sequence alignment program ver. 2.0.5 (Jeanmougin et al. 1998) and the BioEdit program ver. 7.2.5 (Hall 1999) with known genes from other plant species to clarify the phylogenetic relationship of the *VOZ2* gene in citrus. A phylogenetic tree was produced by the neighbor-joining (N-J) method for the deduced amino acid sequences of *VOZ* genes from apple [*Malus*×*domestica* (AB531023, MDP0000729316, MDP0000879912, and MDP0000296843)], *Arabidopsis* (AT1G28520 and AT2G42400), Clementine [*Citrus clementina* (Ciclev10015064m and Ciclev10015076m)], maidenhair fern [*Adiantum capillus-veneris* (KAI5077272)], Lombardy poplar [*Populus nigra* (Potri.004G050900 and Potri.019G092800)], rice [*Oryza sativa* (LOC_Os01g54930 and LOC_Os05g43950)], Satsuma mandarin (LC729264 and LC729265), and sweet

orange [*Citrus sinensis* (XP006467710 and XP006469061)]. The deduced proteins of the TFL1/FT family from plant species used in amino acid comparison are MdFT1 (AB161112) and MdFT2 (AB458504) in apple; AtFT (AT1G65480) and AtTSF (AT4G20370) in *Arabidopsis*; VvFT (DQ871590) in grapevine (*Vitis vinifera*); PnFT1 (AB106111), PnFT1a (AB161109), and PnFT3c (AB110009) in Lombardy poplar; CuFT1 (LC729261) and CuFT3 (LC729263) in Satsuma mandarin; and LeSFT (AY186735) in tomato (*Solanum lycopersicum*). The phylogenetic tree for VOZ2 was displayed using the N-J plot with bootstrap values for 1,000 trials in each branch.

### *Yeast two-hybrid (Y2H) assay*

The *att*B-flanked PCR products for the entire coding regions of *CuVOZ2* or *CuFTs* (*CuFT1* and *CuFT3*) or the truncated region of *CuVOZ2* were introduced into a pDONR221 vector (Invitrogen, Life Technologies Corp., Carlsbad, CA, USA) in-frame as a donor vector. Each entry clone was introduced into a pDEST22 (ampicillin$^{R}$) to construct the expression vector with the GAL4 activation domain (GAL4 AD) (prey). The constructs were designated as CuVOZ2 (AD), CuFT1 (AD) and CuFT3 (AD). The truncations were constructed by gradual deletion of the C-terminal region or deletion of the N-terminal region. The truncated version of CuVOZ2 was designated as CuVOZ2N1 (AD) (1–100aa), CuVOZ2DelN1 (AD) (101–485aa), CuVOZ2N2 (AD) (1–200aa), CuVOZ2N3 (AD) (1–300aa) and CuVOZ2N4 (AD) (1–400aa). Similarly, the constructs produced with pDEST32 (gentamicin$^{R}$) for GAL4 DBD (bait) were designated as CuVOZ2 (BD), CuFT1 (BD) and CuFT3 (BD). Yeast (*Saccharomyces cerevisiae*) strain MaV203 (MAT*α*, *leu*2-3,112, *trp*1-901, *his*3Δ200, *ade*2-101, *gal*4Δ, *gal*80Δ, *SPAL*10::*URA*3, *GAL*1::*lacZ*, *HIS*3$_{\mathrm{UAS\ GAL1}}$::*HIS*3@*LYS*2, *can*1$^{R}$, *cyh*2$^{R}$) (Vidal 1997) was transformed with several combinations of AD and BD plasmids according to the lithium method (Gietz and Woods 2002). Single AD yeast transformants were screened on a selective agar medium with a minimal synthetic defined (SD) base with a –L dropout (DO) supplement (Clontech Laboratories Inc., Mountain View, CA, USA) containing 2% glucose. Single BD transformants were screened on SD –W media. Yeast co-transformed with AD and BD constructs was selected on SD –L/–W media. Co-transformed yeasts were incubated on SD –L/–W/–H media to confirm induction of the *HIS3* gene and the protein–protein interaction. To prevent self-activation of the *HIS3* reporter gene, 25 mM of 3-amino-1,2,4-triazole (3-AT), a *HIS3* inhibitor, was added to the media. The yeasts with the same combination were grown on SD –L/–W/–U media to confirm the activity of the *URA3* reporter gene. For selection against positive interactions, 0.2% 5-fluoroorotic acid (5FOA) was used. All the yeasts were grown at 30°C for 48 h. The protein–protein interactions between CuVOZ2 and CuFTs were also confirmed by the colony filter lift assay.

### *Docking simulation*

The three-dimensional (3D) structure of the proteins and the protein–protein interaction were simulated based on the cDNA sequences of *CuVOZ2*, *CuFT1*, and *CuFT3* to better understand the results obtained in the Y2H system. A deep-learning neural network was applied to predict possible docking regions to understand how CuVOZ2 and CuFTs interact. The protein modeling and interaction were predicted in AlphaFold2_advanced.ipynb (Jumper et al. 2021), a Web-based iPython Notebook service for interactive coding supported by Google. The artificial intelligence predicted and constructed models of protein–protein complex structures using several protein sequence databases and multiple-sequence alignment. The metal ion-binding site was predicted with the help of the Metal Ion-Binding site prediction and modeling server (MIB2) (Lu et al. 2012). Visualizations of protein models and predictions of docking regions were created using ChimeraX ver. 1.5 (Pettersen et al. 2021).

### *Vector construction and* Arabidopsis *transformation*

The oligonucleotide primers of VOZ2_XbaI_F and VOZ2_KpnI_R (Supplementary Table S1) were used to amplify the coding region of *CuVOZ2* to construct a binary vector for plant transformation. The amplified product was digested with *Xba*I and *Kpn*I and cloned into the corresponding restriction enzyme site of the 35SΩ/pSMAK193E plant-transformation vector (Kotoda et al. 2010). The floral-dip method (Clough and Bent 1998) was used to transform wild-type *Arabidopsis* with *Agrobacterium tumefaciens* EHA101. Kanamycin-resistant transgenic seedlings were transplanted from the plate to moistened soil (vermiculite : perlite = 1 : 1) at the two-leaf stage and incubated in a growth chamber (Biotron; Nippon Medical and Chemical Instruments Co., Ltd.) at 22°C under long-day (LD) conditions (16 h photoperiod; cool white fluorescent light, 72.36 $\mu$mol m$^{-2}$ s$^{-1}$). Transgenic plants with an empty vector of pSMAK251 (indicated as PSM251) were used as the control. Morphological and expression analyses were performed on the third-generation ($T_3$) transgenic plants. The number of days to bolting and flowering was tracked. Rosette and cauline leaves were counted at flowering time. The length of the first inflorescence was measured at flowering and 40 days after incubation (DAI). The branches, siliques, nodes, and internodes were also counted or measured 40 DAI. An entire transgenic or control plant was collected for qRT-PCR analysis.

### *Expression analysis in the Satsuma mandarin 'Aoshima' and transgenic* Arabidopsis

Expression analysis of *CuVOZ2* was carried out via qRT-PCR. One microgram of RNA was used to synthesize the first-strand cDNA in 20 $\mu$l of a reaction mixture using a ReverTra Ace® qPCR RT Master Mix (TOYOBO). One microliter of the first-strand cDNA was used as a template in SYBR® Green RealTime PCR Master Mix (TOYOBO) for a total volume of 12.5 $\mu$l. The qRT-PCR was performed using a LightCycler® 96 System (Roche Diagnostics, Mannheim, Germany) as follows: 95°C for 1 min, 40 cycles of 95°C for 15 s and 60°C for 1 min for *CuVOZ2*, *CuActin*, and *AtTUB4*. Three technical replicates were

maintained for each analysis. *CuActin* was used as a reference gene to normalize the transcript levels of *CuVOZ2* (Kotoda et al. 2016). *AtTUB4* was used as a reference gene to normalize the transcript levels of *CuVOZ2* in transgenic *Arabidopsis*. The primer sets used in the experiment are listed in Supplementary Table S1.

### *Statistical analysis*

Data on the number of days to bolting and flowering; the numbers of leaves, nodes, and siliques; and the length of the first inflorescence and internodes were analyzed using one-way ANOVA, and the multiple comparison was done by Tukey's honestly significant difference (HSD) test. Statistical analyses were performed at the significance level of $p<0.05$ using RStudio v.1.2.5089 (RStudio Team 2020).

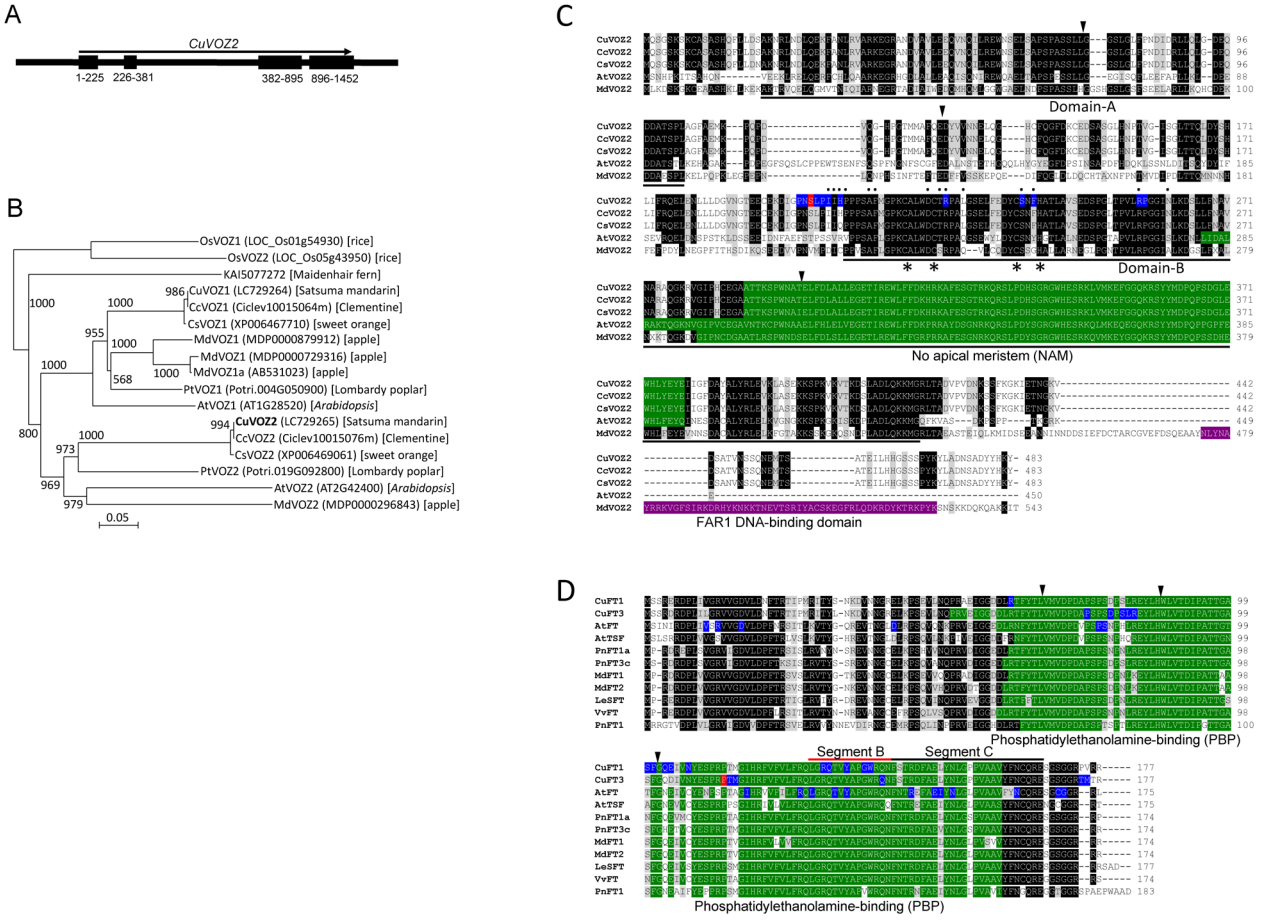


Figure 1. Phylogenetic analysis of *CuVOZ2* and comparison of the deduced protein sequences of VOZ2 or FT in several plant species. (A) Schematic representation of the genomic organization of *CuVOZ2*. The numbers that appear below the exon region are based on the cDNA sequence of *CuVOZ2*. (B) Relationship of the predicted VOZ-family proteins between Satsuma mandarin and other plant species. Phylogenetic tree of VOZ-family proteins of apple, *Arabidopsis*, citrus, maidenhair fern, poplar, rice, and tomato species. The amino acid sequences of *Arabidopsis* VOZ-family proteins were obtained from TAIR, and others were obtained from NCBI, phytozome and Genome Database for Rosaceae (GDR). Numbers along the branches are bootstrap values (1,000 replicates). The unit for the scale bars indicates branch lengths (0.05 substitutions/site). (C) The deduced protein sequence of CuVOZ2 with those of the VOZ2 family proteins from apple, *Arabidopsis*, and citrus species. The genes used for comparison are *MdVOZ2* (MDP0000296843, apple), *AtVOZ2* (AT2G42400, *Arabidopsis*), *CcVOZ2* (Ciclev10015076m, Clementine), *CuVOZ2* (LC729265, Satsuma mandarin), and *CsVOZ2* (XP006469061, sweet orange). Amino acids in black and gray are identical and similar, respectively. The dashes indicate the lack of amino acids. The triangles show the intron positions. The green and purple regions show the predicted motif regions. Two domains, Domain A and Domain B were represented by black lines, defined by Mitsuda et al. (2004). Asterisks represent conserved residues possibly forming a functional zinc-coordinating motif (Mitsuda et al. 2004). Amino acids in blue are in the predicted docking regions when CuVOZ2 interacts with CuFTs. Amino acids with a dot on the top are the amino acid residues predicted to bind with AtFT. The amino acids in red are the amino acid residues predicted to have a hydrogen bond. (D) The deduced protein sequences of CuFT1 and CuFT3 with those of the TFL1/FT family from apple, *Arabidopsis*, grapevine, and Lombardy poplar species. The genes used for analysis are as follows: *MdFT1* (AB161112, apple), *MdFT2* (AB458504, apple), *AtFT* (AT1G65480, *Arabidopsis*), *AtTSF* (AT4G20370, *Arabidopsis*), *VvFT* (DQ871590, grapevine), *PnFT1* (AB106111, Lombardy poplar), *PnFT1a* (AB161109, Lombardy poplar), *PnFT3c* (AB110009, Lombardy poplar), *CuFT1* (LC729261, Satsuma mandarin), *CuFT3* (LC729263, Satsuma mandarin), and *LeSFT* (AY186735, tomato). Putative amino acid sequences were aligned using the ClustalX2 multiple-sequence alignment program ver.2.0.5 (Jeanmougin et al. 1998). Red and black lines on the fourth exon of FT family proteins indicate segment B and C regions, respectively, as defined by Ahn et al. (2006).

## Results

### *Isolation of* CuVOZ2 *from the Satsuma mandarin 'Aoshima'*

The cDNA of *CuVOZ2* was isolated from the Satsuma mandarin 'Aoshima' and the function of the gene was investigated. The *CuVOZ2* gene consisted of four exons of 225, 156, 514, and 557 base pairs (bp) encoding a putative protein of 483 amino acids, which was also confirmed by next-generation sequencing (NGS) of the 'Aoshima' genome (Figure 1A). The length of the coding sequence was 1,452 bp. To investigate the evolutionary link among the *VOZ* genes, a phylogenetic analysis was carried out using the putative amino acid sequences corresponding to *VOZ* genes from apple, *Arabidopsis*, citrus (Clementine, Satsuma mandarin, and sweet orange), maidenhair fern, poplar, and rice. The phylogenetic tree revealed that CuVOZ2 was closely clustered with the VOZ2 of Clementine and sweet orange and with the same clade as AtVOZ2, MdVOZ2, and PtVOZ2 (Figure 1B).

The sequence of CuVOZ2 was 100% identical to that of CcVOZ2, 99.17% identical to that of CsVOZ2 and 53.86% identical to that of previously isolated CuVOZ1 (LC729264) at the amino acid level. The motif search tool using the Pfam database showed that the amino acid sequence of CuVOZ2 contains a C-terminal beta pleated sheet identified as a no apical meristem (NAM) (289–388aa) motif (Finn et al. 2016) (Figure 1C, green regions). One motif, named the phosphoethanolamine-binding protein (PBP), was identified in the latter region in the sequence of TFL1/FT family proteins including CuFT1 (LC729261) and CuFT3 (LC729263) (Figure 1D).

### *Expression pattern of* CuVOZ2

The tissue-specific expression pattern of *CuVOZ2* was examined using qRT-PCR. *CuVOZ2* was expressed in various tissues, as shown in Figure 2. The expression was relatively high in shoot apices in both juvenile and adult phases and stems in the juvenile phase. However, the expression was lower in the reproductive tissues, such as juice sacs and peels in November. The expression was moderate in other tissues at the vegetative and reproductive stages.

### *Interactions of CuVOZ2 with CuFT1 or CuFT3 in the Y2H system*

Auxotrophy assays for *HIS3* and *URA3* reporter genes, sensitivity tests for 5FOA, and X-gal filter lift assays for the *LacZ* reporter gene were performed using the yeast transformants harboring a pair of bait and prey plasmids [CuFT1 (AD)/CuVOZ2 (BD), CuFT1 (BD)/CuVOZ2 (AD), CuFT3 (AD)/CuVOZ2 (BD), and CuFT3 (BD)/CuVOZ2 (AD)] to investigate the protein–protein interactions in the Y2H system. All the yeast

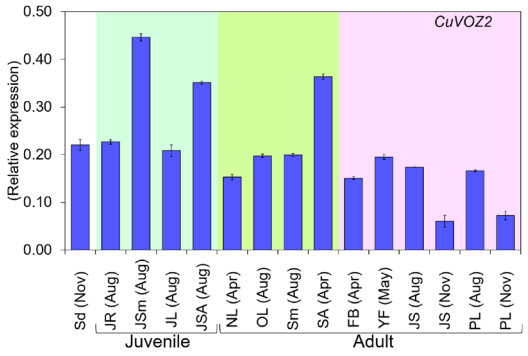


Figure 2. Expression pattern of *CuVOZ2* in various tissues in the Satsuma mandarin 'Aoshima' by quantitative real-time RT-PCR. The samples (left to right) are as follows: the seeds (Sd), juvenile roots (JR), juvenile stems (JSm), leaves from the juvenile plant (JL), and juvenile shoot apices (JSA) of one-year-old seedlings in the juvenile phase; the new leaves in April (NL), old leaves in August (OL), stems with a node in August (Sm), and shoot apices in April (SA) in the adult phase; and the flower buds in April (FB), young fruits in May (YF), juice sacs in August and November (JS), and peels in August and November (PL) in the adult reproductive phase. Expression levels were normalized by citrus actin. Values are the means±SD of the results from three technical replicates. A column without an error bar indicates that the standard deviation fell within the symbol.

constructs that grew on SD –L/–W/–H+25 mM 3-AT showed the induction of the *HIS3* reporter gene in the His auxotrophy assays (Figure 3A). Growth induction of the yeasts containing CuFT1 (AD)/CuVOZ2 (BD) and CuFT3 (AD)/CuVOZ2 (BD) constructs on an SD –L/–W/–U media plate in the Ura auxotrophy assay and growth inhibition of all constructs on an SD –L/–W+5FOA media plate in the 5FOA sensitivity assay confirmed the activity of the *URA3* reporter gene. However, the yeasts containing CuVOZ2 (AD)/CuFT1 (BD) and CuVOZ2 (AD)/CuFT3 (BD) constructs did not show growth induction on the SD –L/–W/–U media plate. The indigo coloration in the X-gal filter assay confirmed the activity of the *LacZ* reporter gene. The growth inhibition of all the BD constructs tested on SD –W or SD –L/–H media plates, and the colony filter lift assay showed that any single constructs were not self-activated (Figure 3B).

### *Identification of binding regions using the Y2H system*

A series of truncated CuVOZ2 proteins were fused with the GAL4 activation domain (GAL4 AD) to identify the region of interaction between CuVOZ2 and CuFT1 (Figure 3C) and between CuVOZ2 and CuFT3 (Figure 3D). In Y2H assays, constructs of the CuVOZ2 truncation series (AD)/CuFTs (BD) showed inhibited growth in the SD –L/–W/–H+25 mM 3-AT media and less blue coloration in the X-gal assay except for the CuVOZ2N4 (AD)/CuFT (BD) constructs. Both the CuVOZ2N4 (AD)/CuFT1 (BD) and CuVOZ2N4 (AD)/CuFT3 (BD) constructs showed normal growth in the

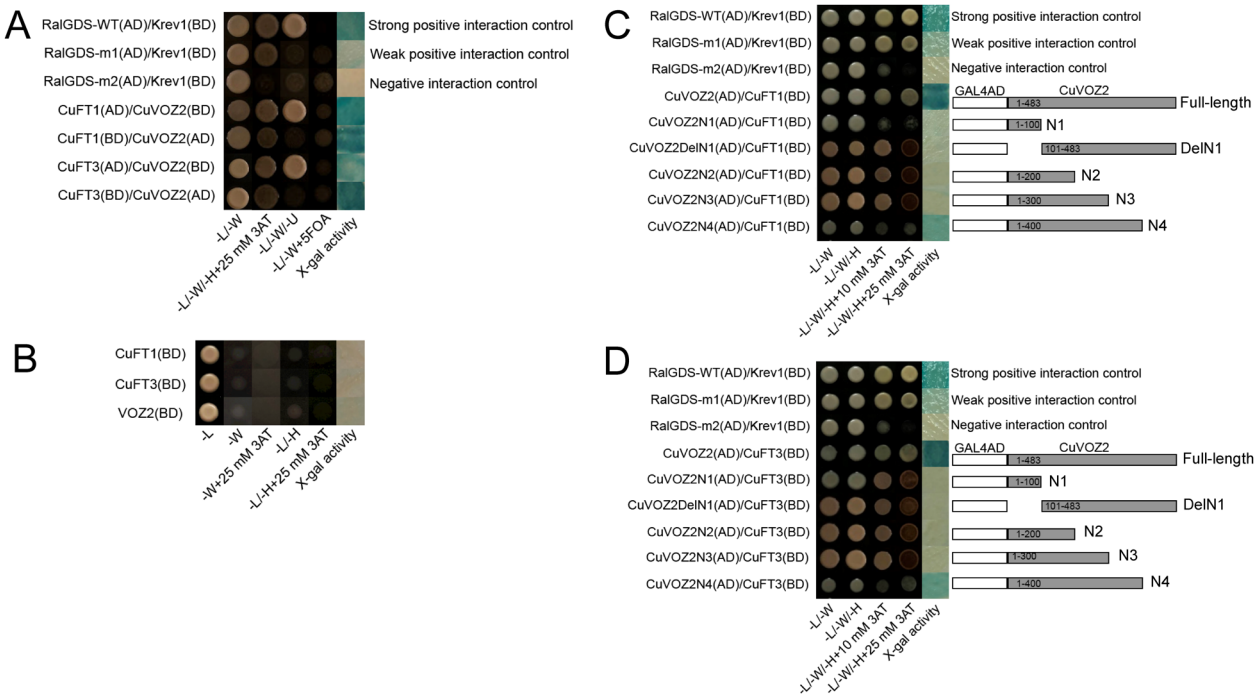


Figure 3. Protein–protein interactions between CuVOZ2 with CuFTs detected in a yeast two-hybrid system. (A) Yeast competent cell MaV203 was transformed with a pair of bait [CuVOZ2(BD) or CuFTs(BD)] and prey [CuVOZ2(AD) or CuFTs(AD)] plasmids, using the lithium method. The transformants were grown at 30°C for 48 h. The selection test for the *HIS3* reporter gene of yeast transformants was performed on a selective agar medium with a Minimal SD Base and –L–W–H DO supplement containing 25 mM 3-amino-1,2,4-triazole (3-AT) and 2% glucose. The selection test for the *URA3* reporter gene was performed on an SD –L/–W/–Ura DO supplement containing 0.2% 5-fluoroorotic acid (5FOA). A subsequent X-gal (5-Bromo-4-chloro-3-indolyl-$\beta$-D-galactopyranoside) filter lift assay for $\beta$-galactosidase activity was performed using yeast transformant cells to test the *LacZ* reporter gene. (B) No effect of self-activation was detected in the constructed vector. The interaction between the truncated CuVOZ2 and full-length CuFT1 (C) and CuFT3 (D) in yeast is shown. The left panels of (C) and (D) show the growth of the transformed yeast cells on SD/–L–W, SD/–L–W–H, SD/–L–W–H+10 mM 3-AT, and SD/–L–W–H+25 mM 3-AT and a filter assay for the $\beta$-galactosidase activity of the transformants grown on SD/–L–W–H. The right panels of (C) and (D) illustrate the full-length or truncated (N1, DelN1, N2–4) version of CuVOZ2. An RalGDS-WT(AD)/Krev1(BD) construct was used as a strong positive interaction control, an RalGDS-m1(AD)/Krev1(BD) construct as a weak positive interaction control, and an RalGDS-m2(AD)/Krev1(BD) construct as a negative interaction control.

SD –L/–W/–H+25 mM 3-AT media, and the indigo coloration in the X-gal assay was similar to that of the full-length CuVOZ2 (AD)/CuFT (BD) constructs. These observations indicated that CuFTs showed little interaction with C-terminal truncations of CuVOZ2 [(N1, 1–100aa), (N2, 1–200aa), and (N3, 1–300aa)] and an N-terminal truncation of CuVOZ2 (DelN1, 101–485aa) on the SD –L/–W/–H+25 mM 3-AT media plate and X-gal assay but showed an apparent interaction with the CuVOZ2N4 region, which consisted of 1–400aa in the N-terminal region (Figure 3C, D).

### *Docking simulation*

The predicted amino acid residues associated with the interaction between CuVOZ2 and CuFT1 in the CuVOZ2–CuFT1 complex were as follows: Pro198, Asn199, Leu201, Ile203, His205, Arg223, Ser236, Phe238, Arg255, and Pro256 in CuVOZ2 (Figures 1C, 4A, B) and Arg62, Ser100, Phe101, Gln103, Glu104, Asn107, Arg130, Gln131, Tyr134, Gly137 and Trp138 in CuFT1 (Figures 1D, 4A, B). The predicted amino acid residues associated with the interaction between CuVOZ2 and CuFT3 in the CuVOZ2–CuFT3 complex were as follows: Ser200, Leu201, Pro202, Ile203, His205, and Phe235 in CuVOZ2 (Figures 1C, 4C, D) and Pro75, Asp79, Ser80, Leu81, Pro113, Thr114, Met115, and Gln140 in CuFT3 (Figures 1D, 4C, D). The common amino acid residues associated with docking in both complexes were Leu201, Ile203, His205, and Phe238 in CuVOZ2 (Figure 1C). No common amino acid residues involved in docking were found for CuFTs. All the predicted amino acid residues of CuVOZ2 involved in docking in the CuVOZ2–CuFT complexes were in the third exon. In the CuVOZ2–CuFT3 complex, one hydrogen bond was observed between the Ser200 of CuVOZ2 and the Pro113 of CuFT3 (Figures 1C, D, 4E). The possibility of the interaction between CuVOZ2 and AtFT in transgenic *Arabidopsis* was also predicted. Ile203, Ile204, His205, Pro206, Ala210, Phe211, Asp220, Thr222, Arg223, Leu226, Ser236, Phe238, Arg256, and Pro257 for CuVOZ2 (Figures 1C, 4F, G) and Val11, Arg13, Asp17, Asp42, Pro77, Ser78, Ile117, Arg126, Leu128, Thr132, Tyr134, Arg145, Glu149, Ile150, Asn152, Asn163, Cys170 and Gly171 for AtFT (Figures 1D, 4F, G) were involved

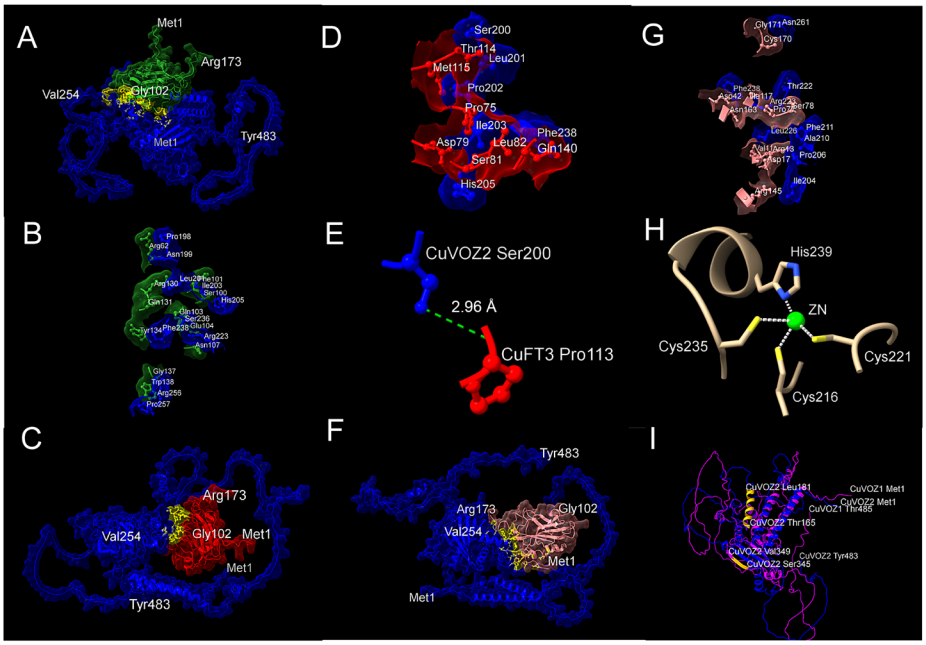


Figure 4. Predicted protein–protein interaction between CuVOZ2 and CuFTs or AtFT. (A) Blue and green areas indicate CuVOZ2 and CuFT1, respectively. (B) The amino acid residues involved in docking in CuVOZ2–CuFT1 complex. (C) Blue and red areas indicate CuVOZ2 and CuFT3, respectively. (D) The amino acid residues involved in docking in CuVOZ2–CuFT3 complex. (E) A predicted hydrogen bond between CuVOZ2 and CuFT3 is shown. (F) Blue and pink areas indicate CuVOZ2 and AtFT, respectively. Met1, Val254, and Tyr483 for CuVOZ2 and Met1, Gly102, and Arg173 for FTs are displayed to confirm the relative position among the complexes. (G) The amino acid residues involved in docking in CuVOZ2–AtFT complex. (H) The predicted $Zn^{2+}$ binding site in the CuVOZ2 protein is shown. (I) Comparative representation of CuVOZ1 and CuVOZ2 proteins. Purple and blue ribbons indicate CuVOZ1 and CuVOZ2, respectively. The orange colored region represents the extra $\alpha$-helix or $\beta$-pleated sheet region on CuVOZ2. The yellow regions in the middle of the two proteins indicate possible docking regions in (A), (C), and (F). The prediction of protein–protein interaction was calculated with AlphaFold.ipynb (Jumper et al. 2021) and visualized with ChimeraX ver. 1.5 (Pettersen et al. 2021). The $Zn^{2+}$ binding site was predicted using the Metal Ion-Binding site prediction and modeling server (MIB2) (Lu et al. 2012). Some amino acids might be hidden in the background.

in the interaction in the protein complexes. The $Zn^{2+}$ ion binding site for CuVOZ2 was predicted in the third exon, consisting of Cys216, Cys221, Cys235, and His239 (Figure 4H). Ten $\alpha$-helices and five $\beta$-pleated sheets were found in the CuVOZ1 protein, whereas CuVOZ2 had 11 $\alpha$-helices and six $\beta$-pleated sheets (Figure 4I).

### *Analysis of* CuVOZ2 *in transgenic* Arabidopsis

The constitutive expression construct of 35SΩ:*CuVOZ2* (Figure 5A) was introduced into wild-type *Arabidopsis* to elucidate the possible role of *CuVOZ2* in transgenic *Arabidopsis* using the heterologous system. About 30 independent transgenic lines were obtained. The $T_3$ transgenic plants were grown in an incubator under LD conditions, and five independent lines ($n$=14) were phenotyped together with the controls (Figure 5B). In addition to the phenotypic analyses, the transgene expression in five independent lines was confirmed via qRT-PCR. All transgenic lines with 35SΩ:*CuVOZ2* expressed the transgene. Among the transgenic plants, lines 2 and 9 showed higher expression as compared to lines 1, 4, and 10 (Figure 5C). Several parameters were taken into consideration to analyze the characteristics of transgenic *Arabidopsis*. 35SΩ:*CuVOZ2* induced early flowering in all transgenic lines (Figure 5B, D). The inflorescence was significantly elongated in lines 1, 9, and 10 at flowering and in lines 2 and 9 40 DAI (Figure 5E). The number of branches in line 1 was higher, whereas that of line 10 was lower (Figure 5F). The number of siliques in lines 1, 2, 4, and 9 was significantly higher (Figure 5G). Significant difference was not observed in the number of nodes for transgenic lines 1, 2, and 4 (Figure 5H), whereas the length of internodes in transgenic lines 2 and 10 was significantly higher (Figure 5I). The number of rosette or cauline leaves did not show any significant differences at flowering time except in one line as compared with the control (Figure 5J, K). The lines with a higher expression of the transgene showed a phenotype of significantly early flowering, long inflorescence, more siliques, and long internodes.

## Discussion

Although Jensen et al. (2010) classified VOZ as a member of NAC family subgroup VIII-2, Gao et al. (2018) classified VOZ genes as an independent gene family. In the VOZ-family, to date, 635 members have been identified in 166 plant species and listed in PlantTFDB, a plant TF database (Jin et al. 2017; Tian et al. 2020). The exon/intron structural diversity plays a crucial role in the evolution of plant gene

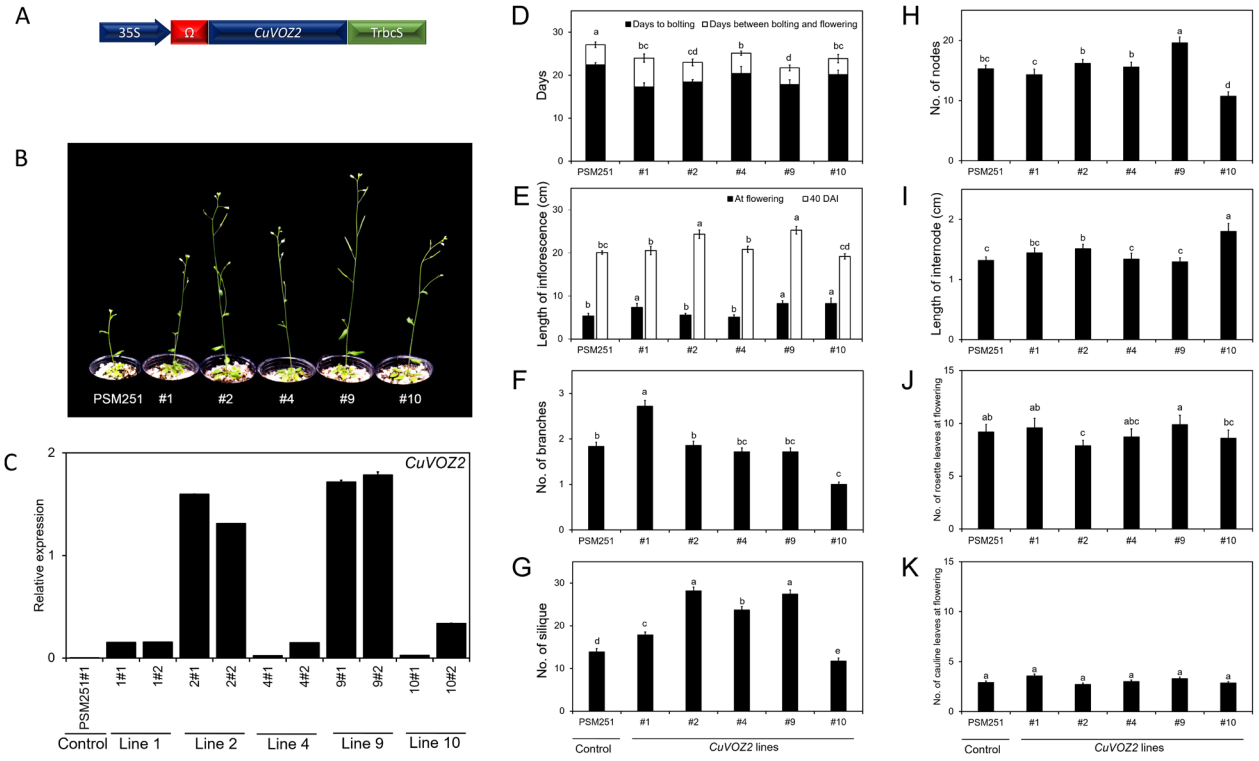


Figure 5. Characterization of transgenic *Arabidopsis* ectopically expressing *CuVOZ2*. (A) Schematic representation of a constructed transformation vector. 35S, promoter region of cauliflower mosaic virus 35S; Ω, Ω sequence responsible for enhancing translation (Gallie and Walbot 1992); and TrbcS, 3′ region of *Arabidopsis rbcS-2B* gene. (B) Typical phenotypes of transgenic *Arabidopsis* with *CuVOZ2* at flowering time in a growth chamber under LD conditions. (C) Expression analysis for transgenes in whole plants of transgenic *Arabidopsis*. The photo was taken on the 22 days after incubation (DAI). Samples for expression analysis of *CuVOZ2* in transgenic lines were collected 40 DAI. PSM251 was the transgenic control plant with an empty vector. Levels of detected amplicons were normalized by reference to *AtTUB4*. (D) Days to bolting and flowering, (E) length of the first inflorescence, (F) no. of branches, (G) no. of siliques, (H) no. of nodes, (I) length of internodes, (J) no. of rosette leaves, and (K) no. of cauline leaves. The transgenic plants in the third generation ($T_3$) and the controls were grown under LD conditions ($n$=14). Days to bolting and flowering were counted from the first day of incubation. All the transgenic plants showed early bolting and flowering. The length of the primary inflorescences was measured at flowering and 40 DAI. The rosette and cauline leaves were counted on the day of the first flowering. Different letters at the top of each column indicate significant differences among the lines, contrasted with Tukey's multiple comparison test ($p$<0.05). Values are the means±SD of the results from three technical replicates per line.

families (Long et al. 1995; Xu et al. 2012). Similarly to *AtVOZ2*, the genomic DNA of *CuVOZ2* was comprised of four exons and three introns in the coding regions (Figure 1A). To analyze the evolutionary connections of 17 putative *VOZ* genes from various species, including the isolated *CuVOZ2* gene from the Satsuma mandarin, a phylogenetic tree was generated based on the deduced amino acid sequences. The phylogenetic tree revealed that CuVOZ2 was closely clustered with the VOZ2 of the Clementine and sweet orange and with the same clade as AtVOZ2, although the similarities between CuVOZ2 and AtVOZ1 and between CuVOZ2 and AtVOZ2 were 61% and 57%, respectively. Interestingly, CuVOZ2 seems to be more closely related to VOZ1 proteins of dicots rather than to VOZ proteins of monocots such as rice (Figure 1B). The differentiation of VOZ1 and VOZ2 transcription factors seems to have occurred after the divergence of monocotyledons and dicotyledons (Shi et al. 2022). These results indicated that CuVOZ2 might have functioned like AtVOZ2 (Figure 1B).

Different VOZ-family members contained highly conserved domains that might be closely related to their identical or similar regulatory functions (Koguchi et al. 2017). No apical meristem (NAM) motif (PF02365) was identified in the VOZ-family genes during the motif search (Figure 1C). The NAM motif was found commonly in both CuVOZ1 and CuVOZ2. On the other hand, CuVOZ2 did not have a DUF4749 (PF15936) motif (Finn et al. 2016), the characteristic feature of CuVOZ1 (LC729264) (Figure 1C; Hasan et al. 2023).

*CuVOZ2* was expressed in various tissues of the Satsuma mandarin (Figure 2). The expression was higher in vegetative tissues (especially juvenile and adult shoot apices and the juvenile stem) than in reproductive tissues. On the other hand, *CuFT1* is expressed exclusively in juice sacs and peels, and CuFT3 is expressed mainly in juvenile roots, adult leaves and apices, and peels (Hasan et al. 2023). According to the report of Nishikawa et al. (2007), *CiFT1*, corresponding to *CuFT1*, is expressed exclusively in juice sacs and peels, and *CiFT3*, corresponding to *CuFT3*, is expressed in vegetative tissues, such as the adult stem

and leaves. *CuVOZ2* was co-expressed in the tissues where *CuFT1*/*CiFT1* and/or *CuFT3*/*CiFT3* were expressed (Figure 2). *AtVOZ2*, coding a vacuolar $H^+$-pyrophosphatase (V-PPase) promoter-binding protein, is expressed in roots, shoots, leaves, flowers, siliques, and suspension cultures in *Arabidopsis* (Mitsuda et al. 2004). The expression pattern of *CuVOZ2* was similar to that of *AtVOZ2* in that both genes were expressed preferentially in roots, shoots, flower buds, and siliques/fruit. AtVOZ1 and AtVOZ2 act as positive regulators of plant flowering by modulating and interacting with CONSTANS (CO), and they are able to bind to the *cis*-acting region of the *A. thaliana* V-PPase gene (*AVP1*), which regulates auxin-mediated organ development and enhances NaCl and drought tolerance (Gaxiola et al. 2001; Kumar et al. 2018; Li et al. 2005; Prasad et al. 2018; Yasui and Kohchi 2014). The *AVP1* expression was increased by the upregulation of *VOZ1* in the transgenic soybean (Han et al. 2021), assuming that the VOZ2–FT protein complexes may affect the activity of V-PPase and/or the function of FT and play an additional role in flower/fruit development and ripening.

A VOZ protein was reported for the first time to interact with FT proteins in apple (Mimida et al. 2011). In citrus, Hasan et al. (2023) reported that CuVOZ1 interacted with CuFTs. In this study, CuVOZ2 from the Satsuma mandarin also exhibited protein–protein interaction with CuFTs in the Y2H system similarly to CuVOZ1 (Figure 3A). Strong positive interactions were confirmed in yeast cells with the combinations of CuFT1 (AD)/CuVOZ2 (BD) and CuFT3 (AD)/CuVOZ2 (BD). Swapping AD and BD could alter the steric force between the proteins and affect the N-terminal region (Chen et al. 2010); hence, the opposite combination of AD and BD may have shown weak interaction in the Y2H system as shown in the previous study (Hasan et al. 2023). The binding region between two proteins was investigated using a truncation series of CuVOZ2 as AD and full-length CuFTs as BD constructs. The truncated construct containing N-terminal 400 amino acids of CuVOZ2 showed a detectable protein–protein interaction between CuVOZ2 and CuFTs (Figure 3C, D). Based on the results of the truncation series, it was suggested that the region from the 1st to 400th amino acid of CuVOZ2 was required, at least for the successful interaction.

Besides the Y2H, simulations predicting 3D models of CuVOZ2–CuFT1 and CuVOZ2–CuFT3 complexes were performed to validate the results of the Y2H assay (Figure 4). Ten amino acid residues in the third exon of CuVOZ2 were involved in docking with CuFT1, and six amino acid residues in the same region were involved in docking with CuFT3 in the CuVOZ2–CuFT1 and CuVOZ2–CuFT3 complexes, respectively (Figure 1C). No amino acid residues were found in NAM motif regions involved in docking in CuVOZ2–CuFT1 and CuVOZ2–CuFT3 complexes. Four amino acids involved in binding with CuFTs, Leu201, Ile203, His205, and Phe238, were common in the third exon of CuVOZ2. The difference in the position of associated amino acids between CuFT1 and CuFT3 might be explained by the difference in their 3D structures, leading to the functional divergence of CuFT1 and CuFT3. The AtVOZ proteins have two distinct conserved regions, N-terminal Domain A, including a stretch of amino acids, and a C-terminal Domain B, also known as the VOZ domain. The third exon of AtVOZ1 and AtVOZ2 contains the zinc-coordination motif with three conserved cysteines and one histidine residue that is required for the DNA-binding and dimerization of VOZ family proteins (Mitsuda et al. 2004). In CuVOZ2, the $Zn^{2+}$ would stabilize the fold by binding with four amino acid residues, Cys216, Cys221, Cys235, and His239, in the zinc-coordination motif with predicted molecular distances of 2.11–2.63 Å (Figure 4H). The predicted residues involved in the interaction between CuVOZ2 and CuFTs were found in the VOZ domain region of CuVOZ2 (Figures 1C, 3C, D, 4A–D), suggesting that the CuVOZ2–CuFT complexes might affect the DNA binding function in CuVOZ2.

The amino acid residues of CuFTs involved in the interactions were found mainly in the PBP motif region. The distance between the residues was predicted to be 1.09–4.37 Å, suggesting that the interaction forces between CuVOZ2 and CuFTs or AtFT in the CuVOZ2–CuFT or CuVOZ2–AtFT complexes were weak Van der Waals forces (Figures 1C, D, 4A–G). A hydrogen bond with a distance of 2.96 Å was found between CuVOZ2 Ser200 and CuFT3 Pro113 in CuVOZ2–CuFT3 complexes (Figures 1C, D, red marked residues; 4E) unlike in the CuVOZ1–CuFT complexes. Based on this prediction, the interaction between CuVOZ2 and CuFT3 might be stronger than those in other complexes. In contrast with CuVOZ1–CuFT complexes (Hasan et al. 2023), CuVOZ2–CuFT complexes did not limit the interacting residues to the fourth exon of CuFTs (Figure 1D). The simulation of the interaction between CuVOZ2 and AtFT also demonstrated that the interacting residues dispersed more than those in CuVOZ1–AtFT complex (Figure 1D). These results imply that the sites of the interaction between CuVOZ2 and CuFTs were not restricted to the fourth exon of CuFTs, where the segments B and C defined by Ahn et al. (2006) are included.

In our previous study, the 35SΩ:*CuVOZ1* transgenic lines showed early bolting, precocious flowering, increased numbers of branches, siliques, nodes, rosette and cauline leaves, and elongated flower stalks with adventitious fertile flowers (Hasan et al. 2023). On the other hand, the 35SΩ:*CuVOZ2* transgenic lines showed early bolting and flowering with an elongated stem with fertile flowers and increased numbers of siliques but no adventitious flower buds (Figure 5). It is noteworthy

that the internodes of the 35SΩ:*CuVOZ2* transgenic lines were extended unlike those of the 35SΩ:*CuVOZ1* transgenic lines (Figure 5I). The differences in the phenotype between 35SΩ:*CuVOZ2* and 35SΩ:*CuVOZ1* transgenic lines might be due to the presence or absence of DUF-4749 motif in the N-terminal region and/or low identity/similarity in amino acid sequences between them. The 3D protein structures of CuVOZ1 and CuVOZ2 were different in the coordination of $\alpha$-helices and $\beta$-pleated sheets. The number of $\alpha$-helices and $\beta$-pleated sheets in CuVOZ1 was ten and five, whereas CuVOZ2 had 11 and six, respectively (Figure 4I). This difference in protein structure might also be a cause of the differences in phenotypes.

The role of *AtVOZ*s in flowering, concerning *CO*, *FLC*, *MAF*, and *PHYTOCHROME B* (*PHYB*), was previously explained in the studies conducted with a double mutant (*voz1 voz2*) in *Arabidopsis* (Celesnik et al. 2013; Kumar et al. 2018; Yasui et al. 2012). The early flowering and other specific phenotypes of 35SΩ:*CuVOZ2* transgenic lines might result from the alteration of *FT* expression because CuVOZ2 showed protein–protein interaction with AtFT in simulation (Figure 4F, G). *AtVOZ1* and *AtVOZ2* suppress *FLC* and act together with *CO* by interacting physically to control flowering (Kumar et al. 2018; Yasui et al. 2012). The downregulation of *FLC* and/or the stabilization of *CO* in transgenic *Arabidopsis* could be another reason for early flowering. *VOZ1* genes in the soybean showed a significant alteration in expression levels in response to dehydration and salt stress treatments, whereas *VOZ2* genes showed a weak change (Li et al. 2020). Light is a key environmental factor affecting flowering time (Zeevaart 1976). The presence of *cis*-acting binding elements, such as LTR, MYB, MBS, ABRE, the CGTCA motif, and the W-box, including a light-related element, Box-4, was reported in the promoter region of *VOZ1/2* from soybeans (*Glycine max* and *G. soja*) and tef (*Eragrostis tef*) (Luo et al. 2020; Mulat and Sinha 2022; Rehman et al. 2021). These studies indicate that *VOZ* TFs might be required to regulate flower induction through some factors, such as abiotic stresses and light. There is a possibility that the stabilized *CuVOZ2* functions as one of the triggers inducing flowering, elongating the inflorescence and internode, and increasing the number of siliques with a consistent result of expression analysis (Figure 5).

The VOZs are also shown to have a function in seed germination. A recent study showed that PHYTOCHROME INTERACTING FACTOR1 (PIF1) induces the expression of *AtVOZ1* and *AtVOZ2* in the dark (Luo et al. 2020). Although both AtVOZ1 and AtVOZ2 were reported to interact with PHYB and promote flowering (Yasui et al. 2012), AtVOZ2 was found to bind to the promoter of a GA biosynthetic gene, *GIBBERELLIN 3-OXIDASE1* (*GA3ox1*) in vitro and in vivo and to directly repress *GA3ox1* in *Arabidopsis*, thereby negatively regulating *PHYB*-mediated seed germination (Luo et al. 2020). The *ga3ox1 Arabidopsis* mutant has a semi-dwarf phenotype (Mitchum et al. 2006), opposite to the phenotype of 35SΩ:*CuVOZ2*. It can be assumed that *CuVOZ2* did not repress but increased active GAs in transgenic *Arabidopsis*. The relationship between GA biosynthesis and *CuVOZ2* remains to be studied.

## Conclusion

The protein–protein interactions between CuVOZ2 and CuFTs were confirmed in this study through a Y2H system. The N-terminal 1st to 400th region of CuVOZ2 was suggested via a truncation experiment to be necessary for the interaction with CuFTs. Furthermore, the 3D structures of the proteins, the nature of interactions, the specific residues involved in docking, and the $Zn^{2+}$ binding site were predicted by virtual simulations. Interestingly, the amino acid residues associated with binding to CuVOZ2 were not exactly the same between CuFT1 and CuFT3. The phenotypes of transgenic *Arabidopsis* with 35SΩ:*CuVOZ2* was similar to those of 35SΩ:*CuVOZ1*, but they differed in that the 35SΩ:*CuVOZ2* lines showed extended internodes and did not produce adventitious flower buds on the elongated flower stalks, whereas 35SΩ:*CuVOZ1* lines showed more branching. *CuVOZ2* might trigger the early flowering and elongation of inflorescence like *CuVOZ1*, but the difference in the phenotypes between the transgenic lines with each gene might partly be due to the variation in the mode of interaction between CuVOZs and other proteins such as FTs. These findings would provide us with an understanding not only of the function of *CuVOZ2* but also of the functional divergence of *CuFT1* and *CuFT3* or *CuVOZ1* and *CuVOZ2* in citrus. The relationship between the protein complexes and the phytohormones, such as abscisic acid and GAs, and the response of the protein complexes to environmental stimuli and/or stresses remains to be studied further.

### Acknowledgements

We are grateful to the staff of Analytical Research Center for Experimental Sciences, Saga University, for technical assistance. We also thank Dr. H. Ichikawa for providing the binary vectors, pSMAK251 and pSMAK193E, and Dr. E. E. Hood for providing *Agrobacterium tumefaciens* EHA101.

### Author contribution

NH, NT, and TN did experiments, NH and NK designed experiments, NH and NK wrote the paper, and NK acquired research funds.

## Funding

This study was supported by a Grant-in-Aid for scientific research from the Ministry of Education, Culture, Sports, Science and Technology (16K07598, 20K06018).

## Conflict of interest

The authors declare that they have no known competing financial interests or personal relationships that could have appeared to influence the work reported in this paper.

## Description of Supplementary Files

Supplementary Table S1. Primer sets used in gene cloning, Y2H, quantitative real-time RT-PCR analysis, and vector construction.

## References

Abe M, Kobayashi Y, Yamamoto S, Daimon Y, Yamaguchi A, Ikeda Y, Ichinoki H, Notaguchi M, Goto K, Araki T (2005) FD, a bZIP protein mediating signals from the floral pathway integrator FT at the shoot apex. *Science* 309: 1052–1056

Ahn JH, Miller D, Winter VJ, Banfield MJ, Lee JH, Yoo SY, Henz SR, Brady RL, Weigel D (2006) A divergent external loop confers antagonistic activity on floral regulators FT and TFL1. *EMBO J* 25: 605–614

Albrigo LG, Stelinski LL, Timmer LW (2019) *Citrus, 2nd edition*. CABI, Boston, MA, pp 1–314

An H, Roussot C, Suárez-López P, Corbesier L, Vincent C, Piñeiro M, Hepworth S, Mouradov A, Justin S, Turnbull C, et al. (2004) CONSTANS acts in the phloem to regulate a systemic signal that induces photoperiodic flowering of *Arabidopsis*. *Development* 131: 3615–3626

Andrés F, Coupland G (2012) The genetic basis of flowering responses to seasonal cues. *Nat Rev Genet* 13: 627–639

Bradley D, Ratcliffe O, Vincent C, Carpenter R, Coen E (1997) Inflorescence commitment and architecture in *Arabidopsis*. *Science* 275: 80–83

Celesnik H, Ali GS, Robison FM, Reddy ASN (2013) *Arabidopsis thaliana* VOZ (Vascular plant One-Zinc finger) transcription factors are required for proper regulation of flowering time. *Biol Open* 2: 424–431

Chen YC, Rajagopala SV, Stellberger T, Uetz P (2010) Exhaustive benchmarking of the yeast two-hybrid system. *Nat Methods* 7: 667–668

Clough SJ, Bent AF (1998) Floral dip, a simplified method for *Agrobacterium*-mediated transformation of *Arabidopsis thaliana*. *Plant J* 16: 735–743

Corbesier L, Vincent C, Jang S, Fornara F, Fan Q, Searle I, Giakountis A, Farrona S, Gissot L, Turnbull C, et al. (2007) FT protein movement contributes to long-distance signaling in floral induction of *Arabidopsis*. *Science* 316: 1030–1033

Finn RD, Coggill P, Eberhardt RY, Eddy SR, Mistry J, Mitchell AL, Potter SC, Punta M, Qureshi M, Sangrador-Vegas A, et al. (2016) The Pfam protein families database, towards a more sustainable future. *Nucleic Acids Res* 44(D1): D279–D285

Gallie DR, Walbot V (1992) Identification of the motifs within the tobacco mosaic virus 5′-leader responsible for enhancing translation. *Nucleic Acids Res* 20: 4631–4638

Gao B, Chen M, Li X, Liang Y, Zhu F, Liu T, Zhang D, Wood AJ, Oliver MJ, Zhang J (2018) Evolution by duplication: Paleopolyploidy events in plants reconstructed by deciphering the evolutionary history of VOZ transcription factors. *BMC Plant Biol* 18: 256

Gaxiola RA, Li J, Undurraga S, Dang LM, Allen GJ, Alper SL, Fink GR (2001) Drought- and salt-tolerant plants result from overexpression of the AVP1 $H^+$-pump. *Proc Natl Acad Sci USA* 98: 11444–11449

Gietz RD, Woods RA (2002) Transformation of yeast by lithium acetate/single-stranded carrier DNA/polyethylene glycol method. In: Guthrie C, Fink GR (eds) *Methods in Enzymology 350*. Academic Press, New York, pp 87–96

Hall TA (1999) BioEdit: A user-friendly biological sequence alignment editor and analysis program for Windows 95/98/NT. *Nucleic Acids Symp Ser* 41: 95–98

Han X, Wang D, Song D (2021) Expression of a maize *SOC1* gene enhances soybean yield potential through modulating plant growth and flowering. *Sci Rep* 11: 12758

Hasan N, Tokuhara N, Noda T, Kotoda N (2023) Citrus VASCULAR PLANT ONE-ZINC FINGER1 (VOZ1) interact with CuFT1 and CuFT3, affecting flowering in transgenic *Arabidopsis*. *Sci Hortic (Amsterdam)* 310: 111702

Jaeger KE, Wigge PA (2007) FT protein acts as a long-range signal in *Arabidopsis*. *Curr Biol* 17: 1050–1054

Jeanmougin F, Thompson JD, Gouy M, Higgins DG, Gibson TJ (1998) Multiple sequence alignment with Clustal X. *Trends Biochem Sci* 23: 403–405

Jensen MK, Kjaersgaard T, Nielsen MM, Galberg P, Petersen K, O'Shea C, Skriver K (2010) The *Arabidopsis thaliana* NAC transcription factor family, structure–function relationships and determinants of ANAC019 stress signalling. *Biochem J* 426: 183–196

Jin J, Tian F, Yang DC, Meng YQ, Kong L, Luo J, Gao G (2017) PlantTFDB 4.0: Toward a central hub for transcription factors and regulatory interactions in plants. *Nucleic Acids Res* 45(D1): D1040–D1045

Jumper J, Evans R, Pritzel A, Green T, Figurnov M, Ronneberger O, Tunyasuvunakool K, Bates R, Žídek A, Potapenko A, et al. (2021) Highly accurate protein structure prediction with AlphaFold. *Nature* 596: 583–589

Koguchi M, Yamasaki K, Hirano T, Sato MH (2017) Vascular plant one-zinc-finger protein 2 is localized both to the nucleus and stress granules under heat stress in *Arabidopsis*. *Plant Signal Behav* 12: e1295907

Koornneef M, Hanhart CJ, van der Veen JH (1991) A genetic and physiological analysis of late flowering mutants in *Arabidopsis thaliana*. *Mol Gen Genet* 229: 57–66

Kotoda N, Hayashi H, Suzuki M, Igarashi M, Hatsuyama Y, Kidou S, Igasaki T, Nishiguchi M, Yano K, Shimizu T, et al. (2010) Molecular characterization of *FLOWERING LOCUS T*-like genes of apple (*Malus*×*domestica* Borkh.). *Plant Cell Physiol* 51: 561–575

Kotoda N, Matsuo S, Honda I, Yano K, Shimizu T (2016) Isolation and functional analysis of two gibberellin 20-oxidase genes from Satsuma mandarin (*Citrus unshiu* Marc.). *Hortic J* 85: 128–140

Kotoda N, Wada M, Komori S, Kidou S, Abe K, Masuda T, Soejima J (2000) Expression pattern of homologues of floral meristem identity genes *LFY* and *AP1* during flower development in apple. *J Am Soc Hort Sci* 125: 398–403

Krajewski AJ, Rabe E (1995) Citrus flowering, a critical evaluation. *J Hortic Sci* 70: 357–374

Kumar S, Choudhary P, Gupta M, Nath U (2018) VASCULAR PLANT ONE-ZINC FINGER1 (VOZ1) and VOZ2 interact with CONSTANS and promote photoperiodic flowering transition. *Plant Physiol* 176: 2917–2930

Li B, Zheng JC, Wang TT, Min DH, Wei WL, Chen J, Zhou YB, Chen M, Xu ZS, Ma YZ (2020) Expression analyses of soybean VOZ transcription factors and the role of GmVOZ1G in drought and salt stress tolerance. *Int J Mol Sci* 21: 2177

Li J, Yang H, Ann Peer W, Richter G, Blakeslee J, Bandyopadhyay A, Titapiwantakun B, Undurraga S, Khodakovskaya M, Richards EL, et al. (2005) *Arabidopsis* $H^+$-PPase AVP1 regulates auxin-mediated organ development. *Science* 310: 121–125

Lin MK, Belanger H, Lee YJ, Varkonyi-Gasic E, Taoka KI, Miura E, Xoconostle-Cázares B, Gendler K, Jorgensen RA, Phinney B, et al. (2007) FLOWERING LOCUS T protein may act as the long-distance florigenic signal in the cucurbits. *Plant Cell* 19: 1488–1506

Liu L, Liu C, Hou X, Xi W, Shen L, Tao Z, Wang Y, Yu H (2012) FTIP1 is an essential regulator required for florigen transport. *PLoS Biol* 10: e1001313

Liu L, Zhu Y, Shen L, Yu H (2013) Emerging insights into florigen transport. *Curr Opin Plant Biol* 16: 607–613

Long M, Rosenberg C, Gilbert W (1995) Intron phase correlations and the evolution of the intron/exon structure of genes. *Proc Natl Acad Sci USA* 92: 12495–12499

Lu CH, Lin YF, Lin JJ, Yu CS (2012) Prediction of metal ion–binding sites in proteins using the fragment transformation method. *PLoS One* 7: e39252

Luo D, Qu L, Zhong M, Li X, Wang H, Miao J, Liu X, Zhao X (2020) Vascular plant one-zinc finger 1 (VOZ1) and VOZ2 negatively regulate phytochrome B-mediated seed germination in *Arabidopsis*. *Biosci Biotechnol Biochem* 84: 1384–1393

Mathieu J, Warthmann N, Küttner F, Schmid M (2007) Export of FT protein from phloem companion cells is sufficient for floral induction in *Arabidopsis*. *Curr Biol* 17: 1055–1060

Mimida N, Kidou SI, Iwanami H, Moriya S, Abe K, Voogd C, Varkonyi-Gasic E, Kotoda N (2011) Apple FLOWERING LOCUS T proteins interact with transcription factors implicated in cell growth and organ development. *Tree Physiol* 31: 555–566

Mitchum MG, Yamaguchi S, Hanada A, Kuwahara A, Yoshioka Y, Kato T, Tabata S, Kamiya Y, Sun TP (2006) Distinct and overlapping roles of two gibberellin 3-oxidases in Arabidopsis development. *Plant J* 45: 804–818

Mitsuda N, Hisabori T, Takeyasu K, Sato MH (2004) VOZ; Isolation and characterization of novel vascular plant transcription factors with a one-zinc finger from *Arabidopsis thaliana*. *Plant Cell Physiol* 45: 845–854

Mulat MW, Sinha VB (2022) VOZS identification from TEF [*Eragrostis tef* (Zucc.) Trotter] using in silico tools decipher their involvement in abiotic stress. *Mater Today Proc* 49: 3357–3364

Nakai Y, Fujiwara S, Kubo Y, Sato MH (2013a) Overexpression of *VOZ2* confers biotic stress tolerance but decreases abiotic stress resistance in *Arabidopsis*. *Plant Signal Behav* 8: e23358

Nakai Y, Nakahira Y, Sumida H, Takebayashi K, Nagasawa Y, Yamasaki K, Akiyama M, Ohme-Takagi M, Fujiwara S, Shiina T, et al. (2013b) Vascular plant one-zinc-finger protein 1/2 transcription factors regulate abiotic and biotic stress responses in Arabidopsis. *Plant J* 73: 761–775

Nishikawa F, Endo T, Shimada T, Fujii H, Shimizu T, Omura M, Ikoma Y (2007) Increased *CiFT* abundance in the stem correlates with floral induction by low temperature in Satsuma mandarin (*Citrus unshiu* Marc.). *J Exp Bot* 58: 3915–3927

Notaguchi M, Abe M, Kimura T, Daimon Y, Kobayashi T, Yamaguchi A, Tomita Y, Dohi K, Mori M, Araki T (2008) Long-distance, graft-transmissible action of *Arabidopsis* FLOWERING LOCUS T protein to promote flowering. *Plant Cell Physiol* 49: 1645–1658

Ohshima S, Murata M, Sakamoto W, Ogura Y, Motoyoshi F (1997) Cloning and molecular analysis of the *Arabidopsis* gene *Terminal Flower 1*. *Mol Gen Genet* 254: 186–194

Pettersen EF, Goddard TD, Huang CC, Meng EC, Couch GS, Croll TI, Morris JH, Ferrin TE (2021) UCSF ChimeraX: Structure visualization for researchers, educators, and developers. *Protein Sci* 30: 70–82

Prasad KVSK, Xing D, Reddy ASN (2018) Vascular plant one-zinc-finger (VOZ) transcription factors are positive regulators of salt tolerance in *Arabidopsis*. *Int J Mol Sci* 19: 3731

Putterill J, Varkonyi-Gasic E (2016) FT and florigen long-distance flowering control in plants. *Curr Opin Plant Biol* 33: 77–82

Rehman SU, Qanmber G, Tahir MHN, Irshad A, Fiaz S, Ahmad F, Ali Z, Sajjad M, Shees M, Usman M, et al. (2021) Characterization of Vascular plant One-Zinc finger (VOZ) in soybean (*Glycine max* and *Glycine soja*) and their expression analyses under drought condition. *PLoS One* 16: e0253836

RStudio Team (2020) RStudio: Integrated Development for R. RStudio, PBC, Boston, MA. URL: http://www.rstudio.com/ (Accessed Nov 21st, 2022)

Samach A, Onouchi H, Gold SE, Ditta GS, Schwarz-Sommer Z, Yanofsky MF, Coupland G (2000) Distinct roles of CONSTANS target genes in reproductive development of *Arabidopsis*. *Science* 288: 1613–1616

Shi P, Jiang R, Li B, Wang D, Fang D, Yin M, Yin M, Gu M (2022) Genome-wide analysis and expression rofiles of the VOZ gene family in quinoa (*Chenopodium quinoa*). *Genes (Basel)* 13: 1695

Song C, Lee J, Kim T, Hong JC, Lim CO (2018) VOZ1, a transcriptional repressor of DREB2C, mediates heat stress responses in *Arabidopsis*. *Planta* 247: 1439–1448

Tamaki S, Matsuo S, Wong HL, Yokoi S, Shimamoto K (2007) Hd3a protein is a mobile flowering signal in rice. *Science* 316: 1033–1036

Tian F, Yang DC, Meng YQ, Jin J, Gao G (2020) PlantRegMap: Charting functional regulatory maps in plants. *Nucleic Acids Res* 48(D1): D1104–D1113

Vidal M (1997) The reverse two-hybrid system. In: Bartel RL, Fields S (eds) *The Yeast Two-Hybrid System*. Oxford University Press, New York, pp 109–147

Wang J, Wang R, Fang H, Zhang C, Zhang F, Hao Z, You X, Shi X, Park CH, Hua K, et al. (2021) Two VOZ transcription factors link an E3 ligase and an NLR immune receptor to modulate immunity in rice. *Mol Plant* 14: 253–266

Wigge PA (2011) FT, a mobile developmental signal in plants. *Curr Biol* 21: R374–R378

Wigge PA, Kim MC, Jaeger KE, Busch W, Schmid M, Lohmann JU, Weigel D (2005) Integration of spatial and temporal information during floral induction in *Arabidopsis*. *Science* 309: 1056–1059

Xu G, Guo C, Shan H, Kong H (2012) Divergence of duplicate genes in exon–intron structure. *Proc Natl Acad Sci USA* 109: 1187–1192

Yasui Y, Kohchi T (2014) *VASCULAR PLANT ONE-ZINC FINGER1* and *VOZ2* repress the *FLOWERING LOCUS C* clade members to control flowering time in *Arabidopsis*. *Biosci Biotechnol Biochem* 78: 1850–1855

Yasui Y, Mukougawa K, Uemoto M, Yokofuji A, Suzuri R, Nishitani A, Kohchi T (2012) The phytochrome-interacting VASCULAR PLANT ONE–ZINC FINGER1 and VOZ2 redundantly regulate flowering in *Arabidopsis*. *Plant Cell* 24: 3248–3263

Zeevaart JAD (1976) Physiology of flower formation. *Annu Rev Plant Physiol* 27: 321–348